Probing equilibrium by nonequilibrium dynamics: Aging in Co/Cr superlattices

T. Mukherjee,[1] M. Pleimling,[2] and Ch. Binek[1,*]
[1]*Department of Physics & Astronomy and the Nebraska Center for Materials and Nanoscience, University of Nebraska–Lincoln, Lincoln, Nebraska 68588-0111, USA*
[2]*Department of Physics, Virginia Polytechnic Institute and State University, Blacksburg, Virginia 24061-0435, USA*
(Received 9 July 2010; revised manuscript received 18 September 2010; published 14 October 2010)

Magnetization relaxation is investigated in a structurally ordered magnetic Co/Cr superlattice. Tailored nanoscale periodicity creates mesoscopic spatial magnetic correlations with slow relaxation dynamics when quenching the system into a nonequilibrium state. Magnetization transients are measured after exposing the heterostructure to a magnetic set field for various waiting times. Scaling analysis reveals an asymptotic power-law behavior in accordance with a full aging scenario. The temperature dependence of the relaxation exponent shows pronounced anomalies at the equilibrium phase transitions of the antiferromagnetic superstructure and the ferromagnetic to paramagnetic transition of the Co layers. The latter leaves only weak fingerprints in the equilibrium magnetic behavior but gives rise to a prominent change in nonequilibrium properties. Our findings suggest scaling analysis of nonequilibrium data as a probe for weak equilibrium phase transitions.

DOI: 10.1103/PhysRevB.82.134425 PACS number(s): 75.70.−i, 05.70.Ln, 75.30.Kz, 81.40.Cd

I. INTRODUCTION

Nonequilibrium thermodynamics is one of today's active frontiers in fundamental science.[1] Particularly appealing are some of the unifying aspects of systems far from equilibrium when considered against the background of the evermore specializing fields of the physical, chemical, and biological sciences. Spin-glass physics and its relation to concepts of memory and pattern recognition in biological neural networks is one example for transdisciplinarity of nonequilibrium statistical mechanics.[2,3] Progress in experiment and theory of statistical mechanics is needed to push the boundaries of the understanding of nonequilibrium properties of complex systems even further.

Magnetic model systems serve traditionally as workhorses in equilibrium statistical mechanics.[4,5] They maintain their importance in the challenging field of nonequilibrium thermodynamics. Magnetic aging phenomena are conceptually simple with well-defined experimental protocols. At the same time, even macroscopically complex magnetic behavior can be described by simple model Hamiltonians. Similarly to the celebrated concept of universality in equilibrium statistical mechanics where symmetry of the interactions and dimensionality unify otherwise microscopically different systems into classes with common critical behavior, there are magnetic control parameters grouping microscopically distinct model systems into classes with universal aspects of nonequilibrium thermodynamics.

II. SUPERLATTICES FOR TAILORED SPIN-SPIN CORRELATION

Magnetic multilayer thin films and their controlled growth via modern molecular beam epitaxy (MBE) methodology provide experimental access to a wide range of microscopic parameters. Superlattice structures allow tailoring the intralayer and interlayer exchange as well as the spin-fluctuation spectra through geometrical confinement. We tailor those properties in Co/Cr thin-film superlattices to study magnetic aging phenomena in the framework of scaling analysis. For example, the Curie temperature of the Co constituent films can be tailored between $0 < T_C^{Co}(d) \leq 1388$ K by geometrical confinement through variation in the film thickness, d.[6,7] Cr spacer layers provide antiferromagnetic (AF) exchange coupling between these Co films. The oscillating thickness dependence of the Ruderman-Kittel-Kasuya-Yoshida-type interlayer exchange becomes tunable in strength through control of the Cr interlayer film thickness.[8–10]

III. MAGNETIC RELAXATION IN ORDERED MAGNETIC SYSTEMS

Magnetization relaxation in weakly correlated spin systems is typically a fast process on a laboratory time scale since it depends on the microscopic spin-flip time of about 10^{-8} s.[11] From an experimental point of view, it is convenient to study magnetic relaxation phenomena on a time scale from seconds to hours. However, this requires the presence of nonexponentially decaying spin-spin correlation. Glassy systems in general and spin glasses, in particular, provide experimental access to a nonergodic regime below the glass transition temperature where the dynamics of the system becomes very slow in comparison with the microscopic spin-flip time. The magnetic glass properties with their slow spin dynamics require disorder and frustration in the magnetic interactions. While disordered glassy systems have been extensively studied, only little work has been done on the relaxation of ordered magnetic systems.[12] With rare exceptions,[13] experimental investigations in ordered bulk systems face the problem of fast dynamics. The situation improves when taking advantage of an analogy of the phenomenon of critical slowing down with the spin dynamics in ordered magnetic nanostructures. Critical slowing down is observed when entering the critical regime of a, e.g., magnetic second-order phase transition. Here, on approaching the critical temperature, the diverging magnetic correlation length gives rise to diverging relaxation times. However, the smallness of the critical regime makes it almost impossible

to experimentally observe this phenomenon in ordered bulk systems.[14]

Our distinct approach to study magnetic relaxation in ordered magnetic systems builds on the increase in the characteristic spin-spin correlation length in comparison to atomic bulk systems when taking advantage of magnetic nanostructuring. We use magnetic superlattices, structured on the nanoscale, to increase relaxation times when replacing atomic spins through mesoscopically correlated regions. More specifically, we grow three-dimensional artificial AF superlattices of two-dimensional ferromagnetic (FM) Co films with in-plane anisotropy coupling antiferromagnetically perpendicular to the plane across Cr spacer layers.[15] As a result, we obtain temperature-dependent magnetic metastability and slow relaxation dynamics in the absence of disorder and frustration. Our experimental results on magnetic aging can be interpreted in the framework of a dynamic scaling analysis which is based on the assumption of a full aging scenario.[1,16] This scenario predicts asymptotic power-law relaxation, $M(t,S) \propto S^{-a}(t/S)^{-\lambda/z}$, with nonuniversal exponents a and λ/z. Here z is the dynamical exponent that governs the algebraic growth of the time-dependent correlation length. The exponents a and λ, the latter being sometimes called the autoresponse exponent, are nonequilibrium exponents that describe the dynamical scaling behavior of the response in the asymptotic aging regime.[1]

Here we evidence the correlation between anomalies in the temperature dependence of λ/z vs T with magnetic equilibrium phase transitions. λ/z vs T reveals the breakdown of three-dimensional AF order at the Néel temperature, $T_N(H=0)$, followed by a transition at T_C from FM order of the uncorrelated Co films to global paramagnetism of the sample. The latter transition is very weakly pronounced in the equilibrium magnetic data but creates a prominent drop of about 60% in λ/z at T_C. These findings pave the way to probe particularly equilibrium phase transitions via pronounced nonequilibrium properties.

IV. RESULTS AND ANALYSIS

Figure 1 shows the temperature dependence, M vs T, of the magnetic moment, M, of our Cr(10 nm)/[Co(0.60 nm)/Cr(0.78 nm)]$_{20}$/Cr(2 nm) heterostructure. The data are taken with the help of a superconducting quantum interference device (SQUID MPMS-XL, Quantum Design) on field heating (FH) and field cooling (FC) in $\mu_0 H=5$ [solid triangles (FH) and circles (FC)] and 30 mT [open triangles (FH) and circles (FC)] in-plane magnetic fields after initial zero-field cooling (ZFC). The ZFC-FH/FC branches of the 5 mT $M_{\text{ZFC-FH}}$ vs T/M_{FC} vs T, exhibit pronounced irreversibilities close to $T_N(\mu_0 H=5\ \text{mT})=53$ K of the superlattice. In analogy to atomic bulk antiferromagnets, homogeneously applied magnetic fields weaken the AF order parameter and reduce the AF ordering temperature such that $T_N=T_N(H)$, where $T_N(H)$ is given by the inflection point of $M_{\text{ZFC-FH}}$ vs T.[17] This field dependence is seen in Fig. 1 in the decrease from $T_N(\mu_0 H=5\ \text{mT})=53$ K to $T_N(\mu_0 H=30\ \text{mT})=25$ K.

The Co/Cr superlattice periodicity of 1.4 nm is evidenced in Fig. 1(a) via small-angle x-ray diffraction measured with

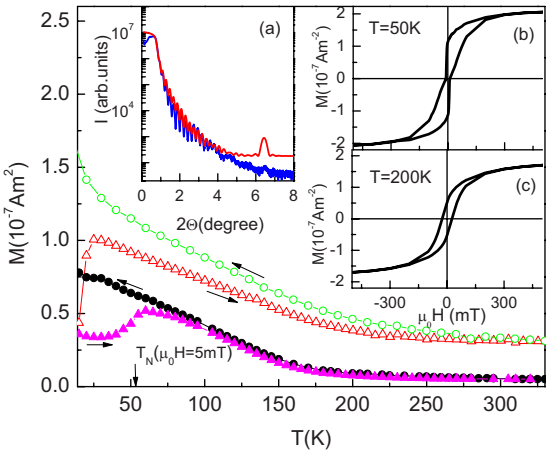

FIG. 1. (Color online) ZFC-FH and FC M vs T data measured in $\mu_0 H=5$ [solid triangles (FH) and circles (FC)] and 30 mT [open triangles (FH) and circles (FC)]. $T_N(\mu_0 H=5\ \text{mT})=53$ K is indicated by a vertical arrow. Inset (a) shows small-angle x-ray diffraction data (blue lower line) and the corresponding simulation (red upper line). Inset (b) shows a hysteresis loop, M vs H, measured at $T=50$ K. Inset (c) shows the corresponding hysteresis loop at $T=200$ K.

the help of characteristic Cu $K\alpha$ radiation of wavelength $\lambda_{\text{Cu}\,K\alpha}=0.1544$ nm. A superstructure peak appears in the data at $2\theta=6.5°$ (blue lower line) and is reproduced by simulation (red upper line). Details of the structural analysis including wide angle x-ray diffraction can be found in Ref. 15.

Figure 1(b) shows an isothermal magnetization hysteresis loop, M vs H, measured at $T=50\ \text{K} \ll T_N(H=0)$. Contraction of the loop at the coercive fields is a fingerprint of AF coupling.[18,19] Figure 1(c) shows the corresponding hysteresis loop at $T=200\ \text{K} \gg T_N(H=0)$. Here the AF interlayer correlation is thermally broken and, hence, the contraction of the hysteresis loop is absent.[20] This behavior is in close analogy to atomic layered AF systems such as the prototypical metamagnets $FeCl_2$ and $FeBr_2$.[5,21–23]

The insets of Fig. 2 show typical log-log plots of our magnetic aging data measured at $T=20$ (left frame) and 160 K (right frame) below and above the AF transition. The displayed data are five-point adjacent averages. A small homogenizing field of $\mu_0 H=5$ mT, which brings the individual Co layers into single domain states, has been applied on cooling the sample from $T=330$ K down to various target temperatures $20 \leqslant T \leqslant 300$ K where magnetization relaxation is measured, respectively. At each target temperature, the sample is exposed to a set field of $\mu_0 H=30$ mT for various waiting times $S=10$ (squares), 100 (circles), and 1000 s (triangles). After field exposure, the magnetic field is quickly removed on a time scale $\Delta t \approx 1\ \text{s} \ll S$ and isothermal relaxation, M vs t, is recorded using SQUID magnetometry.

Our magnetization transients confirm the asymptotic power-law behavior, $M(t,S) \propto S^{-a}(t/S)^{-\lambda/z}$, when represented in a log-log scaling plot, $S^a M(t,S)$ vs $\propto t/S$ where asymptotic linear behavior with slope λ/z is expected. Optimized exponents $a=1.32\times10^{-3}$, $\lambda/z=1.9\times10^{-3}$ at 20 K and $a=3.0\times10^{-3}$, $\lambda/z=4.3\times10^{-3}$ at 160 K give rise to data collapse on respective master curves (green/light gray lines in Fig. 2) in

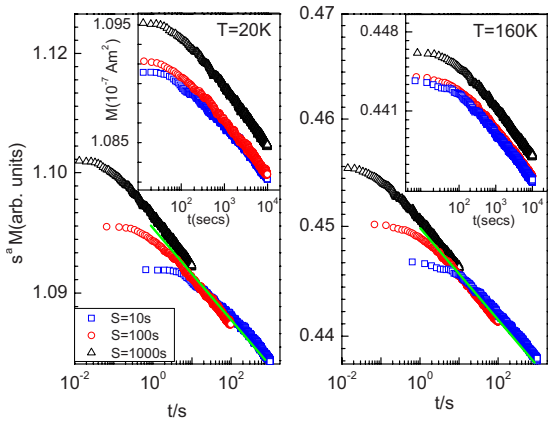

FIG. 2. (Color online) Insets show log-log plots of magnetic aging data, M vs t, measured after cooling in $\mu_0 H=5$ mT, from $T=330$ K to $T=20$ (left frame) and 160 K (right frame) and subsequent exposure to a set field of $\mu_0 H=30$ mT for various waiting times $S=10$ (squares), 100 (circles), and 1000 s (triangles) followed by field removal on a time scale $\Delta t \approx 1$ s $\ll S$. Main frames show the same data in a scaling plot, $S^a M(t,S)$ vs $\propto t/S$ with data collapse in the asymptotic regimes on respective master curves (green/light gray lines).

the asymptotic regime. In accordance with the scaling law, we obtain identical λ/z values for a given temperature at all waiting times within less than 5% error. Note, that without changing λ/z a shift of the master curve along the $S^a M$ axis (away from the middling position) will give rise to virtually perfect collapse with the $S=10$ s relaxation data (Fig. 2 blue squares), which approximate best the approach of the true asymptotic regime for $t/s > 100$. It is the temperature dependence of λ/z which we will discuss below as a nonequilibrium parameter with extreme sensitivity on equilibrium magnetic transitions.

Alternatively, when plotting $F(t)=\frac{M(t,S)-M(t_1,S)}{M(t_2,S)-M(t_1,S)}$ for various waiting times, S, at a given temperature one expects data collapse in the asymptotic regime onto the waiting-time-independent master curve $F(t)=\frac{t^{-\lambda/z}-t_1^{-\lambda/z}}{t_2^{-\lambda/z}-t_1^{-\lambda/z}}$. Here $t_{1,2}$ are two arbitrary but fixed times in the asymptotic regime. Note that the structure of the experimentally motivated scaling function $F(t)$ eliminates the impact of time-independent background signals. In addition, data collapse is achieved through the single parameter λ/z, which can be determined independently from the asymptotic region of the log-log plots of the relaxation data. Note, that attempts to determine λ/z via a single-parameter least-squares fit is not recommended due to the insensitivity of $F(t)$ on variation in λ/z. The inset of Fig. 3 shows a log-log plot of the magnetization transients at $T=140$ K and waiting times $S=10$ (squares), 100 (circles), and 1000 s (triangles). The corresponding scaling plot is shown in log-log representation of $F(t)$ calculated for $t_1=1000$ and $t_2=5000$ s. The green/light gray line is the master curve calculated from $t_{1,2}$ and $\lambda/z=4.6\times10^{-3}$. The residual S dependence at small t is in accordance with the expected breakdown of the scaling law when leaving the asymptotic regime.

Figure 4 represents the culmination of our findings. It evidences a hitherto unexplored bridge between traditional

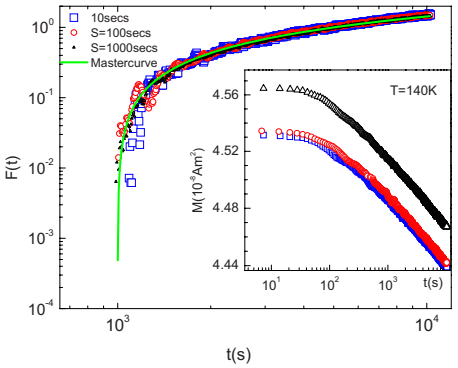

FIG. 3. (Color online) Inset shows a log-log plot of M vs t for $T=140$ K and waiting times $S=10$ (squares), 100 (circles), and 1000 s (triangles). Main frame shows corresponding scaling plot in log-log representation of $F(t)$ (see text) calculated for $t_1=1000$ and $t_2=5000$ s with master curve (green/light gray line).

equilibrium and progressive nonequilibrium thermodynamics. Figure 4 substantiates that we can identify weak equilibrium phase transitions in M vs T via anomalies in the temperature dependence of λ/z. To this end we compare the ZFC-FH/FC M vs T data measured in $\mu_0 H=1$ mT (solid circles) with λ/z vs T (open circles) obtained from the scaling analysis of the relaxation data (see Fig. 2 for typical examples). The vertical line highlights the correlation between the equilibrium AF transition temperature $T_N(\mu_0 H=1$ mT$)=90$ K and the local minimum in λ/z vs T. Note that in theoretical studies of model systems a change in the value of λ/z is routinely observed when approaching a phase transition by changing external parameters.[1] This decrease in $-\lambda/z$ reveals a faster decorrelation of nonequilibrium states

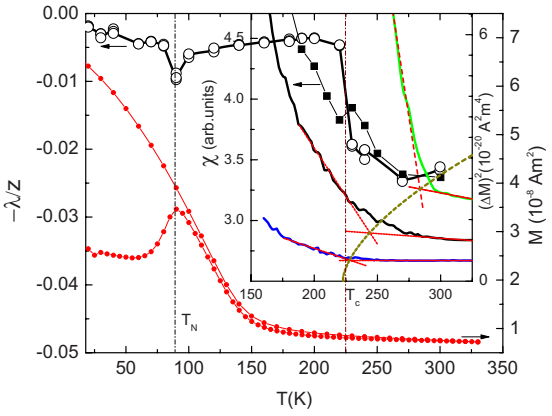

FIG. 4. (Color online) ZFC-FH/FC M vs T equilibrium data measured in $\mu_0 H=1$ mT (solid circles) and λ/z vs T (open circles) obtained from the scaling analysis of the relaxation data. The vertical dashed line highlights $T_N(\mu_0 H=1$ mT$)=90$ K coinciding with the local minimum in λ/z vs T. A second vertical dashed line marks the weak ferromagnetic transition at $T_C \approx 225$ K. The inset displays the dc susceptibility, χ vs T (solid squares), and $(M_{FC}-M_{ZFC\text{-}FH})^2$ vs T, measured at $\mu_0 H=0.1$ (blue lower line), 0.2 (black center line), and 0.4 mT (green/light gray upper line). Linear best fits (red dashed linear lines) intercept at $T_m(H)$, respectively. A power law (dashed dark curved yellow line) extrapolates $T_m(H)$ to $T_m(H=0)=T_C \approx 225$ K.

due to the presence of enhanced fluctuations at different length scales. With increasing temperature, λ/z vs T shows a second, more pronounced, anomaly at $T \approx 225$ K. Note that the λ/z data in the main frame extend continuously into the inset of Fig. 4. An abrupt 60% drop of λ/z vs T is indicated by a second vertical line. Interestingly, at first glance the equilibrium M vs T data appear featureless at this temperature. However, the results of closer inspection of equilibrium isotherms, M vs H and isofields, M vs T, reveal various weak anomalies. The inset of Fig. 4 displays the detailed analysis of the equilibrium data exposing the weak phase transition around 225 K. Note the synchronization of the temperature axes of the main frame and the inset.

First, we determine the dc susceptibility, χ vs T, from the slopes of various magnetization isotherms (not shown) in the vicinity of $H=0$. These χ vs T data are displayed as solid squares in the inset revealing a peak at $T \approx 225$ K. We interpret this peak as a weak singularity of the FM transition of the individual ultrathin Co layers. The rounding results from the finite value of the amplitude $\mu_0 \delta H = \pm 0.5$ mT probing the magnetization response around $H=0$. A strongly reduced T_C of the Co layers in comparison to bulk cobalt ($T_C = 1388$ K) is expected from thickness confinement of the spin correlations and additional interface alloying.[6] This interpretation is strongly supported by additional analysis of various interpolated ZFC-FH/FC M vs T data. The inset shows, $(M_{FC} - M_{ZFC\text{-}FH})^2$ vs T, measured at $\mu_0 H = 0.1$ (blue lower line), 0.2 (black center line), and 0.4 mT (green/light gray upper line). This analysis is motivated by mean-field considerations and the question of what happens to the critical temperature in the presence of a conjugate field lifting criticality. We show that the temperature, T_m, of maximum slope in M vs T at $H>0$ shifts with increasing H toward higher temperatures away from T_C with a power law $H^{2/3}$ fulfilling the condition $\lim_{H\to 0} T_m(H) = T_C$. In the vicinity of T_C, mean-field and Landau theory are equivalent. We thus discuss the Landau free energy $G = \frac{1}{2} a_0 (T - T_C) M^2 + \frac{1}{4} b M^4 - MH$. From $\partial G / \partial M = 0$, we obtain the cubic equation for the equilibrium magnetization $M = M(T,H)$. For further analytic investigation we simplify the latter in the limit $T \approx T_C$ and small magnetic field-induced magnetization. In the spirit of successive approximations we substitute the magnetization in the cubic term through $M = \frac{H}{a_0 (T - T_C)}$. The resulting approximate $M = M(T,H)$ expression allows for the analytic calculation of $\partial^2 M / \partial T^2 = 0$. Its solution with respect to T provides the temperature of maximum slope which reads $T_m(H) = T_C + \frac{(10b)^{1/3}}{a_0} H^{2/3}$.

We determine $T_m(H)$ of our data through analysis of $(M_{FC} - M_{ZFC\text{-}FH})^2$ vs T for various H. Again, motivated by mean-field results where the square of the order parameter is a linear function of temperature, we use linear best fits (red dashed linear lines in inset of Fig. 4) and their intercepts to approximate $T_m(H)$. Since $\lim_{H\to 0} T_m(H) = T_C$ is expected to hold also for our experimental data we extrapolate the intercept temperatures, $T_m(H)$, toward $H=0$ using a power law (dashed dark curved yellow line) and obtain $T_m(H=0) = T_C \approx 225$ K. This extrapolated T_C is in good agreement with the maximum of χ vs T. Most importantly both of these equilibrium signatures coincide with the far more pronounced nonequilibrium λ/z anomaly at $T_C \approx 225$ K.

V. SUMMARY AND CONCLUSIONS

In summary we have shown that equilibrium magnetic phase transitions can strongly affect the nonequilibrium magnetic properties in an ordered nanostructured superlattice. Nanostructuring creates magnetic correlations which bring relaxation times into the experimentally easily accessible domain of seconds to hours. We used an MBE-grown Co/Cr superlattice with antiferromagnetic coupling between ferromagnetic Co layers as a model system with extended temperature regions far from equilibrium. Magnetization transients are analyzed using the theoretically expected scaling function in the aging regime. The scaling exponent has a surprisingly sensitive temperature dependence originating from the subtle temperature dependence of the spin-spin correlations. Our approach has the potential to evolve into a new tool to investigate weak phase transitions in magnetically nanostructured systems with sensitivity hitherto not achieved by equilibrium methodology. In addition, our system should also allow future verifications of detailed theoretical predictions of the scaling forms of nonequilibrium response functions, coming from the theory of local scale invariance.[1]

ACKNOWLEDGMENTS

Financial support by NRI, and NSF through EPSCoR, Career under Grant No. DMR-0547887, and MRSEC under Grants No. 0820521 (C.B.) and No. DMR-0904999 (M.P.).

*cbinek2@unl.edu

[1] M. Henkel and M. Pleimling, *Non-Equilibrium Phase Transitions*, Ageing and Dynamical Scaling Far from Equilibrium Vol. 2 (Springer, Heidelberg, 2010).
[2] J. J. Hopfield, Proc. Natl. Acad. Sci. U.S.A. **79**, 2554 (1982).
[3] J. J. Hopfield, D. I. Feinstein, and R. G. Palmer, Nature (London) **304**, 158 (1983).
[4] L. J. de Jongh and A. R. Miedema, Adv. Phys. **23**, 1 (1974).
[5] Ch. Binek, *Ising-type Antiferromagnets: Model Systems in Statistical Physics and in the Magnetism of Exchange Bias* (Springer, Berlin, 2003).
[6] D. Sellmyer and R. Skomski, *Advanced Magnetic Nanostructures* (Springer, New York, 2005).
[7] F. Huang, M. T. Kief, G. J. Mankey, and R. F. Willis, Phys. Rev. B **49**, 3962 (1994).
[8] P. Grünberg, R. Schreiber, Y. Pang, M. B. Brodsky, and H. Sowers, Phys. Rev. Lett. **57**, 2442 (1986).
[9] H. Zabel, J. Phys.: Condens. Matter **11**, 9303 (1999).
[10] P. Bruno, Phys. Rev. B **52**, 411 (1995).
[11] D. P. Mitra and J. S. S. Whiting, J. Phys. F: Met. Phys. **8**, 2401 (1978).
[12] J. A. Mydosh, *Spin Glasses: An Experimental Introduction* (Tay-

lor & Francis, London, 1993).
[13] R. V. Chamberlin and M. R. Scheinfein, Science **260**, 1098 (1993).
[14] J. Als-Nielsen and R. J. Birgeneau, Am. J. Phys. **45**, 554 (1977).
[15] T. Mukherjee, S. Sahoo, R. Skomski, D. J. Sellmyer, and Ch. Binek, Phys. Rev. B **79**, 144406 (2009).
[16] M. Henkel and M. Pleimling, Phys. Rev. B **78**, 224419 (2008).
[17] M. E. Fisher, Philos. Mag. **7**, 1731 (1962).
[18] S. G. E. te Velthuis, J. S. Jiang, S. D. Bader, and G. P. Felcher, Phys. Rev. Lett. **89**, 127203 (2002).
[19] O. Hellwig, A. Berger, and E. E. Fullerton, Phys. Rev. Lett. **91**, 197203 (2003).
[20] J. U. Thiele, T. Hauet, and O. Hellwig, Appl. Phys. Lett. **92**, 242502 (2008).
[21] Ch. Binek, W. Kleemann, and H. Aruga Katori, J. Phys.: Condens. Matter **13**, L811 (2001).
[22] Ch. Binek, Phys. Rev. Lett. **81**, 5644 (1998).
[23] W. Selke, Z. Phys. B: Condens. Matter **101**, 145 (1996).